

Observation of Ultrahigh-Energy Cosmic Rays with the ANITA Balloon-Borne Radio Interferometer

S. Hoover,¹ J. Nam,² P. W. Gorham,³ E. Grashorn,⁴ P. Allison,³ S. W. Barwick,⁵ J. J. Beatty,⁴ K. Belov,¹ D. Z. Besson,⁶ W. R. Binns,⁷ C. Chen,⁸ P. Chen,^{8,9} J. M. Clem,¹⁰ A. Connolly,¹¹ P. F. Dowkontt,⁷ M. A. DuVernois,^{3,12} R. C. Field,⁹ D. Goldstein,⁵ A. G. Vieregge,¹ C. Hast,⁹ M. H. Israel,⁷ A. Javai,¹⁰ J. Kowalski,³ J. G. Learned,³ K. M. Liewer,¹³ J. T. Link,^{3,14} E. Lusczek,¹² S. Matsuno,³ B. C. Mercurio,⁴ C. Miki,³ P. Miočinović,³ C. J. Naudet,¹³ J. Ng,⁹ R. J. Nichol,¹¹ K. Palladino,⁴ K. Reil,⁹ A. Romero-Wolf,³ M. Rosen,³ L. Ruckman,³ D. Saltzberg,¹ D. Seckel,¹⁰ G. S. Varner,³ D. Walz,⁹ and F. Wu⁵

¹*Department of Physics and Astronomy, University of California, Los Angeles, California 90095, USA*

²*Department of Physics, Ewha Womans University, Seoul, South Korea*

³*Department of Physics and Astronomy, University of Hawaii, Manoa, Hawaii 96822, USA*

⁴*Department of Physics, Ohio State University, Columbus, Ohio 43210, USA*

⁵*Department of Physics, University of California, Irvine, California 92697, USA*

⁶*Department of Physics and Astronomy, University of Kansas, Lawrence, Kansas 66045, USA*

⁷*Department of Physics, Washington University in St. Louis, Missouri 63130, USA*

⁸*Department of Physics, Graduate Institute of Astrophysics & Leung Center for Cosmology and Particle Astrophysics, National Taiwan University, Taipei, Taiwan*

⁹*SLAC National Accelerator Laboratory, Menlo Park, California, 94025, USA*

¹⁰*Department of Physics, University of Delaware, Newark, Delaware 19716, USA*

¹¹*Department of Physics and Astronomy, University College London, London, United Kingdom*

¹²*School of Physics and Astronomy, University of Minnesota, Minneapolis, Minnesota 55455, USA*

¹³*Jet Propulsion Laboratory, Pasadena, California 91109, USA*

¹⁴*Currently at NASA Goddard Space Flight Center, Greenbelt, Maryland, 20771, USA*

(Received 18 May 2010; published 5 October 2010)

We report the observation of 16 cosmic ray events with a mean energy of 1.5×10^{19} eV via radio pulses originating from the interaction of the cosmic ray air shower with the Antarctic geomagnetic field, a process known as geosynchrotron emission. We present measurements in the 300–900 MHz range, which are the first self-triggered, first ultrawide band, first far-field, and the highest energy sample of cosmic ray events collected with the radio technique. Their properties are inconsistent with current ground-based geosynchrotron models. The emission is 100% polarized in the plane perpendicular to the projected geomagnetic field. Fourteen events are seen to have a phase inversion due to reflection of the radio beam off the ice surface, and two additional events are seen directly from above the horizon. Based on a likelihood analysis, we estimate angular pointing precision of order 2° for the event arrival directions.

DOI: [10.1103/PhysRevLett.105.151101](https://doi.org/10.1103/PhysRevLett.105.151101)

PACS numbers: 98.70.Sa, 95.55.Br, 95.55.Vj, 95.85.Ry

The origin of ultrahigh energy cosmic rays (UHECR) remains a mystery decades after their discovery [1,2]. Key to the solution will be increased statistics on events of high enough energy ($\geq 3 \times 10^{19}$ eV) to elucidate both the endpoint region of the UHECR energy spectrum as seen at Earth, and their directional intensity on the sky. The primary difficulty is the extreme rarity of events at these energies. Despite steady progress with experiments such as the Pierre Auger Observatory, there remains room for new methodologies. Cosmic rays have been detected for decades via radio emission from various mechanisms [3–16] but until now, not in this crucial energy range, which offers the possibility of pointing the UHECRs back to their sources. We present data from the Antarctic Impulsive Transient Antenna (ANITA) [17] which represents the first entry of radio techniques into this energy range. We find 16 UHECR events, $\geq 40\%$ of which are above 10^{19} eV, and we show compelling evidence of their

origin as geosynchrotron emission from cosmic ray showers. Our results indicate degree-scale precision for reconstruction of the UHECR arrival direction, lending strong credence to efforts to develop radio geosynchrotron detection as a competitive method of UHECR particle astronomy.

Geosynchrotron emission arises when the electron-positron particle cascade initiated by a primary cosmic ray encounters the Lorentz force in the geomagnetic field. The resulting acceleration deflects the electrons and positrons and they begin to spiral in opposite directions around the field lines [18,19]. In air, the particles' radiation length is of order 40 g cm^{-2} , a kilometer or less at the altitudes of air shower maximum development. Particle trajectories form partial arcs around the field lines before they lose enough energy to drop out of the shower. The meter-scale longitudinal thickness of the shower particle "pancake" is comparable to radio wavelengths below several hundred

MHz; thus the ensemble behavior of all of the cascade particles yields forward-beamed synchrotron emission, which is partially or fully coherent in the radio regime. Therefore, the resulting radio impulse power grows quadratically with primary particle energy, and at the highest energies, yields radio pulses that are detectable at large distances. Current systems under development for detection of these radio impulses are colocated with and triggered by cosmic ray particle detectors on the ground [13–15]. They detect showers with primary energies in the 10^{17} – 10^{18} eV range because of their limited acceptance. No such system has reported a sample of $>10^{19}$ eV UHECR events, nor any events detected solely by radio.

The ANITA long-duration balloon payload is launched from Williams Field, Antarctica. It takes advantage of the stratospheric South Polar Vortex to circle the Antarctic continent at altitudes of 35–37 km while synoptically observing an area of ice of order 1.5×10^6 km². During flight, ANITA records all nanosecond-duration radio impulses over a 200–1200 MHz radio frequency band. The threshold is a few times the received power (~ 10 pW) of thermal emission from the ice. The direction of detected signals, determined by pulse-phase interferometric mapping [Fig. 1, [17]], is localized to an angular ellipse of $0.3^\circ \times 0.8^\circ$ (elevation \times azimuth) which is projected back onto the continent to determine the origin of the pulse. ANITA’s mission is the detection of ultrahigh energy neutrinos via linearly polarized coherent radio Cherenkov pulses from cascades the neutrinos initiate within the ice

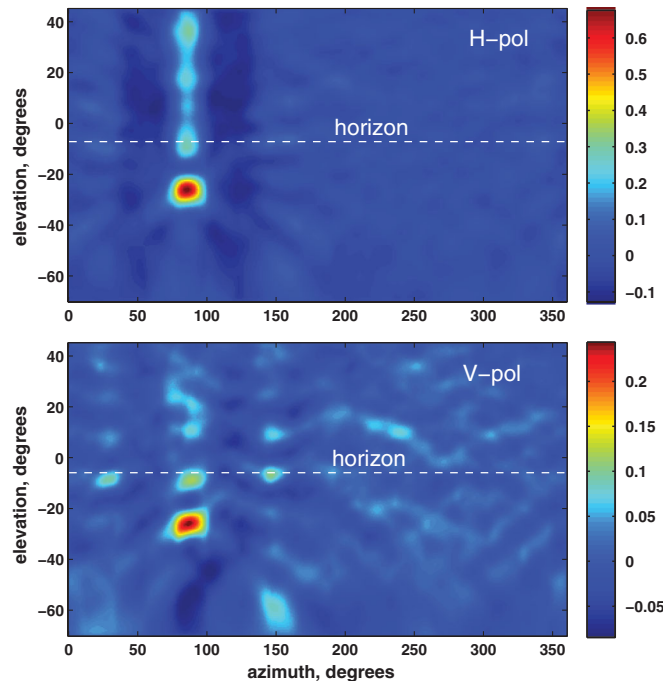


FIG. 1 (color). Interferometric map of relative correlated intensity in H_{pol} (top panel) and V_{pol} (bottom panel) for event 3 623 566, which occurred in a region of Antarctica where the geomagnetic inclination gave an appreciable V_{pol} component. Map details are covered elsewhere [20].

sheets. Virtually all impulsive signals detected during a flight are of anthropogenic origin, but such events can be rejected with high confidence because of their association with known human activity, which is carefully monitored in Antarctica. For its first flight, during the 2006–2007 Austral summer, ANITA’s trigger system was designed to maximize sensitivity to linearly polarized radio pulses, but purposely blinded to the plane of polarization. However, the entire polarization information—both vertical and horizontal (V_{pol} and H_{pol})—was recorded for subsequent analysis. Since radio pulses of neutrino origin strongly favor vertical polarization, due to the geometric-optics constraints on the radio Cherenkov cone as it refracts through the ice surface, we used the H_{pol} information as a sideband test for our blind neutrino analysis.

Our results were surprising: while the neutrino analysis (V_{pol}) gave a null result, a statistically significant sample of 6 H_{pol} events was found initially [20], and a more sensitive analysis now yields 16. These events are randomly distributed around ANITA’s integrated field-of-view [Fig. 2], uncorrelated in location to human activity or to each other, but closely correlated to each other in their radio pulse profile and frequency spectrum [Fig. 3, top panel]. Their measured planes of polarization are found in every case to be perpendicular to the local geomagnetic field [Fig. 4], as expected from geosynchrotron radiation. With two exceptions, the events reconstruct to locations on the surface of the ice; the two exceptional cases have directional origins above the horizon, but below the horizontal (at our altitude, the horizon is about 6° below the horizontal). Earth-orbiting satellites are excluded as a possible source since the nanosecond radio temporal coherence observed is impossible to retain for signals that propagate through the ionospheric plasma, which is highly dispersive in our

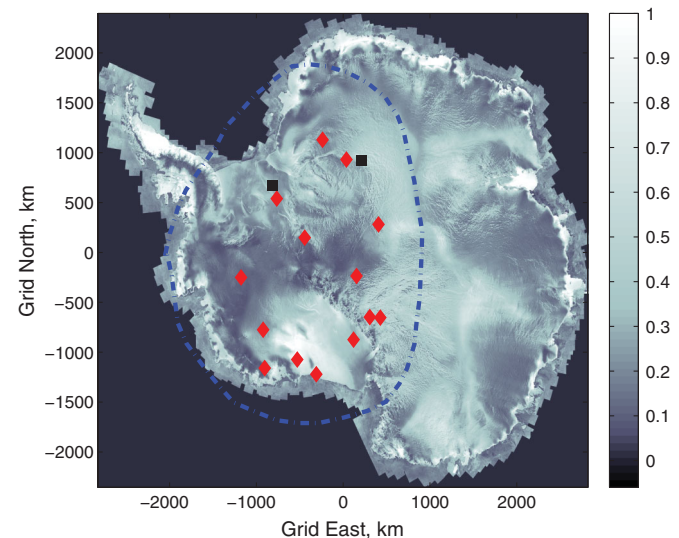


FIG. 2 (color). Map of locations of detected reflected (red diamond) and direct (black square) UHECR events superimposed on a microwave backscatter amplitude map of Antarctica (Radarsat) within our field of view (dash-dotted line).

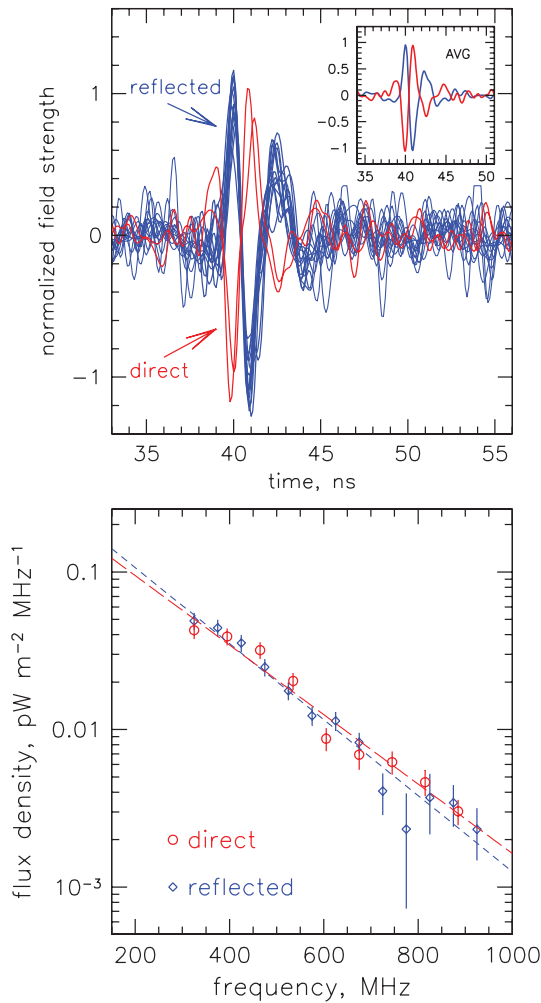


FIG. 3 (color). Top panel: Overlay of the 16 UHECR event H_{pol} pulse shapes, showing the two direct events (red) and 14 reflected events (blue) with inverted phase. Inset: Average pulse profile for all events. Bottom panel: Flux density for both the averaged direct and reflected events, along with fits to an exponential. Errors at low frequency are primarily due to systematic uncertainty in the antenna gains, and to thermal noise statistics at higher frequencies.

frequency regime. The 14 below-horizon events are phase-inverted compared to the two above-horizon events, as expected for specular reflection [Fig. 3, top panel]. From these observations we conclude that ANITA detects a signal, seen in most cases in reflection from the ice sheet surface, which originates in the earth's atmosphere and which involves electrical current accelerating transverse to the geomagnetic field. Such observations are in every way consistent with predictions of geosynchrotron emission from cosmic ray air showers. The robust correlation shown in Fig. 4 is strong evidence that the geosynchrotron radiation from cosmic rays is the dominant emission mechanism in this geometry and frequency range. Since these far-field observations result in a simple plane wave at the detector, these data will provide strong constraints on cosmic ray radio emission models.

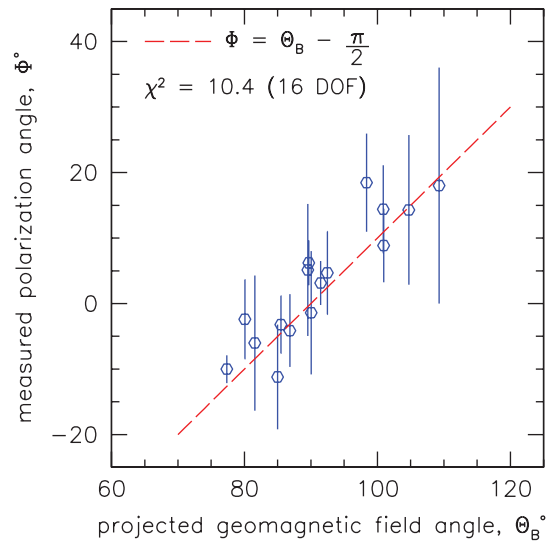


FIG. 4 (color). Plane of polarization of UHECR events compared to the angle of the magnetic field local to the event and Lorentz force expectation (red line). Reflected events are corrected for surface Fresnel coefficients. Angles are from the horizontal.

Our data represent the first broadband far-field measurements of geosynchrotron emission in the ultra high frequency range. The average observed radio-frequency spectral flux density of the above- and below-horizon events, shown in Fig. 3, is consistent with an exponential decrease with frequency, with a mean exponential falloff of $(180 \pm 13 \text{ MHz})^{-1}$ for reflected events and $(197 \pm 15 \text{ MHz})^{-1}$ for direct events. This observation indicates a much flatter decay with frequency than that given by extrapolations from ground-based measurements at lower frequency and parametrizations [21,22]. The lack of any statistically significant difference in the spectra for the direct and reflected events indicates that ice roughness is unimportant for the average surface reflection. To estimate the electric field amplitude at the source of these emissions, we model the surface reflection using standard physical-optics treatments developed for synthetic-aperture radar analysis. Such models use self-affine fractal surface parameters [23] and Huygens-Fresnel integration over the specular reflection region to estimate both amplitude loss and phase distortion from residual slopes or roughness. We used digital elevation models from Radarsat [24] to estimate surface parameters for each of the event reflection points, known to a few km precision. In most cases the surface parameters are found to be smooth, yielding only modest effects on the reflection amplitude; in a minority of the events, surface parameters were estimated to be rougher, but still within the quarter-wave-rms Rayleigh criterion for coherent reflection [25]. Fresnel reflection coefficients were determined using a mean near-surface index of refraction of $n = 1.33$, typical of Antarctic firn.

To estimate the primary energy for the observed events, we used a data-driven maximum likelihood fit to the

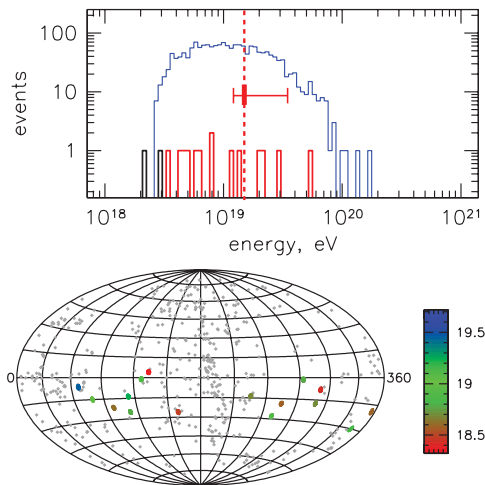


FIG. 5 (color). Top panel: Energies of detected reflected (red) and direct (black) UHECR events, and a simulated reflected event sample (blue). The estimated mean energy and $\pm 2\sigma$ errors are indicated by the vertical dashed line and horizontal bars. Bottom: Map in celestial coordinates (α , δ) of the ANITA events (circles) with error ellipses. Although event energies are 2–10 times lower than required for directional correlation, the map (with nearby Véron-Cetty active galactic nuclei in gray diamonds) is shown to indicate the pointing resolution. The estimated energy [in $\log(E/\text{eV})$] for each event is indicated by color. ANITA’s exposure is approximately uniform across the band $5^\circ > \delta > -30^\circ$.

observed amplitude, phase, and frequency distribution. The fit accounted for the radio emission’s shower energy dependence and angular distribution, along with attenuation due to distance, surface roughness, and reflection from the surface, as well as the known UHECR energy spectrum [1]. The angular distribution and surface roughness utilized physically motivated parametrizations [23,26] and the overall emission scale was drawn from a distribution from literature [12,14,21,27]. The mean energy of the ensemble of reflected events is estimated to be $1.5 \pm 0.4(\text{stat})_{-0.3}^{+2.0}(\text{sys}) \times 10^{19}$ eV, approaching the threshold of the Greisen-Zatsepin-Kuzmin (GZK) suppression [28,29]. For the direct events, the mean energy is lower due to stronger direct signals, but the acceptance—limited to a narrow angular band around the horizon—is also much lower. Figure 5 shows the energies and sky map of the detected events. The large asymmetry in the systematic uncertainty of the energy is due to the uncertainty in the angular offset, which tends to strongly bias towards underestimating the event energy. The fit results imply that the rf signals from these highly inclined, distant showers are significantly stronger than would be predicted by current geosynchrotron models [14,21,27] extrapolated to ANITA’s frequency regime and very different geometry. An attempt to apply these models was not able to reproduce the event rate and observed radio power; further work is in progress.

We estimate a mean angle of observation relative to the true shower axis of $(1.5 \pm 0.5)^\circ$, comparable to that of

ground-based cosmic ray observatories, and adequate to allow us to map these events back to the sky with a final error circle of $\sim 2^\circ$ diameter. The resulting map is shown in Fig. 5. As expected for events in this energy range, the ensemble is uncorrelated to active galactic nuclei in the nearby universe, as intergalactic magnetic deflection is significant assuming our nominal energy scale is correct; the map is shown to illustrate the potential for a larger ANITA-like sample of events and the obtainable angular precision. Estimates from our simulations indicate that, after optimization for UHECR observation, a new 30-day flight of ANITA could detect a total of several hundred geosynchrotron events, with 60–80 above 10^{19} eV, and ~ 10 above the nominal GZK cutoff energy. We conclude that a far-field radio observatory is viable at the highest cosmic ray energies, and if the fidelity of models of the geosynchrotron process continues to improve at the rate it has in recent years, such an approach will be able to further elucidate possible correlations in cosmic ray origin directions as well as the shape of the UHECR energy spectrum in the GZK region.

We are grateful to NASA, the U.S. National Science Foundation, the U.S. Department of Energy, and the Columbia Scientific Balloon Facility for their generous support of these efforts.

-
- [1] J. Abraham *et al.* (Pierre Auger Collaboration), *Phys. Lett. B* **685**, 239 (2010).
 - [2] M. Nagano and A. A. Watson, *Rev. Mod. Phys.* **72**, 689 (2000).
 - [3] J. V. Jelley *et al.*, *Nature (London)* **205**, 327 (1965).
 - [4] N. A. Porter *et al.*, *Phys. Lett.* **19**, 415 (1965).
 - [5] S. N. Vernov *et al.*, *Pis'ma Zh. Eksp. Teor. Fiz.* **5**, 157 (1967) [*JETP Lett.* **5**, 126 (1967)].
 - [6] P. R. Barker, W. E. Hazen, and A. Z. Hendel, *Phys. Rev. Lett.* **18**, 51 (1967).
 - [7] D. J. Fegan and P. J. Slevin, *Nature (London)* **217**, 440 (1968).
 - [8] W. E. Hazen, A. Z. Hendel, H. Smith, and N. J. Shah, *Phys. Rev. Lett.* **22**, 35 (1969).
 - [9] W. E. Hazen, A. Z. Hendel, H. Smith, and N. J. Shah, *Phys. Rev. Lett.* **24**, 476 (1970).
 - [10] R. E. Spencer, *Nature (London)* **222**, 460 (1969).
 - [11] D. J. Fegan and D. M. Jennings, *Nature (London)* **223**, 722 (1969).
 - [12] H. R. Allan, *Progress in Elementary Particles and Cosmic Ray Physics*, edited by J. G. Wilson and S. G. Wouthuysen (North-Holland, Amsterdam, 1971), Vol. 10, pp. 171–304, and references therein.
 - [13] D. Ardouin *et al.*, *Astropart. Phys.* **31**, 192 (2009).
 - [14] S. Nehls *et al.*, *Nucl. Instrum. Methods Phys. Res., Sect. A* **589**, 350 (2008).
 - [15] W. D. Apel (LOPES Collaboration), *Astropart. Phys.* **32**, 294 (2010).
 - [16] H. Falcke *et al.*, *Nature (London)* **435**, 313 (2005).
 - [17] P. W. Gorham *et al.*, *Astropart. Phys.* **32**, 10 (2009).
 - [18] H. Falcke and P. Gorham, *Astropart. Phys.* **19**, 477 (2003).

- [19] D. A. Suprun, P. W. Gorham, and J. L. Rosner, *Astropart. Phys.* **20**, 157 (2003).
- [20] P. W. Gorham *et al.*, *Phys. Rev. Lett.* **103**, 051103 (2009).
- [21] T. Huege and H. Falcke, *Astropart. Phys.* **24**, 116 (2005).
- [22] A. Nigl *et al.*, *Astron. Astrophys.* **488**, 807 (2008).
- [23] M. K. Shepard and B. A. Campbell, *Icarus* **141**, 156 (1999).
- [24] H. Liu, K. Jezek, B. Li, and Z. Zhao, 2001. Boulder, Colorado: National Snow and Ice Data Center. Digital media.
- [25] *Propagation of Radiowaves*, edited by L. Barclay (Institute of Electrical Engineers, London, 2003), 2nd ed..
- [26] J. D. Jackson, *Classical Electrodynamics* (Wiley & Sons, New York, 1975), 2nd ed..
- [27] T. Huege, R. Ulrich, and R. Engel, *Astropart. Phys.* **27**, 392 (2007).
- [28] K. Greisen, *Phys. Rev. Lett.* **16**, 748 (1966).
- [29] G. T. Zatsepin and V. A. Kuzmin, *Pis'ma Zh. Eksp. Teor. Fiz.* **4**, 114 (1966) [*JETP Lett.* **4**, 78 (1966)].